J Mater Sci (2010) 45:2775–2779
DOI 10.1007/s10853-010-4266-1

# Luminescence in rare earth-doped transparent glass ceramics containing $GdF_3$ nanocrystals for lighting applications

**Zhifa Shan · Daqin Chen · Yunlong Yu ·
Ping Huang · Hang Lin · Yuansheng Wang**

Received: 8 October 2009 / Accepted: 26 January 2010 / Published online: 6 February 2010
© Springer Science+Business Media, LLC 2010

**Abstract** Rare earth ions-doped transparent glass ceramics containing hexagonal $GdF_3$ nanocrystals with a mean size of 16 nm were prepared. Energy dispersive x-ray spectroscopy and luminescence spectrum investigation evidenced the incorporation of rare earth ions into $GdF_3$ nanocrystals. The efficient energy transfer from $Gd^{3+}$ to $Tb^{3+}$ was demonstrated in the $Tb^{3+}$-doped glass ceramics, which resulted in an intense green light emission originated from $Tb^{3+}$: $^5D_4 \rightarrow {}^7F_6$ transition via the sensitization of $Gd^{3+}$. Compared with the precursor glass, the $Dy^{3+}$-doped glass ceramic exhibited longer lifetime and lower yellow-to-blue emission intensity ratio owing to the allocation of $Dy^{3+}$ ions in the low-phonon-energy $GdF_3$ environment. Under ultraviolet excitation, the $Dy^{3+}$-doped samples emitted bright white light, indicating their potential application in white light emitting diodes.

## Introduction

Rare earth (RE) ions-doped transparent oxyfluoride glass ceramics, achieved by controlled crystallization of the precursor glass with appropriate chemical composition, have attracted great attention due to their favorable properties benefited from both fluoride crystal and oxide glass matrix, i.e., low phonon energy and high mechanical and chemical stabilities [1–3]. The key factor for the efficient luminescence lies on the partition of the optically active RE ions into the precipitated fluoride nanocrystals [4]. The lanthanide trifluorides nanocrystals embedded glass ceramics are therefore promising materials since the lanthanide ions could be substituted easily by RE ions of the same valence. In addition, the lanthanide trifluorides have low phonon energy that makes them possible to reduce the undesirable non-radiative de-excitation of RE ions [5–10]. Recently, the preparation and the luminescent properties of the RE-doped $LaF_3$ and $YF_3$ nanocrystals embedded glass ceramics have been well studied [11, 12]. Unlike $La^{3+}$ and $Y^{3+}$, $Gd^{3+}$ could be used as the sensitizer for $Sm^{3+}$, $Eu^{3+}$, $Eu^{2+}$, and $Tb^{3+}$ in some materials [13, 14]. However, to our knowledge, few investigations on the optical behaviors of the RE-doped glass ceramics containing $GdF_3$ nanocrystals were reported so far.

In recent years, there has been an increasing trend for the white light emitting diodes (W-LEDs) to replace the conventional incandescent and fluorescent lamps for their advantages in energy saving and related environmental benefits. At present, W-LEDs are usually fabricated by combination of a blue LED chip with fluorescence phosphors [15]. However, the difference between the individual degradation rates of the blue LED chip and the phosphors coated on the chip would cause a chromatic aberration and a poor white light performance. To solve this problem, it is essential to develop novel materials that could emit bright white light under ultraviolet (UV) chip excitation [16, 17]. In this case, the UV excitation light is invisible and could be totally absorbed by phosphors. In the scheme of constructing current W-LEDs, epoxy resin is used to mix the phosphor powder to enable its coating on the chip, which may shorten the lifetime of the LED owing to unavoidable aging of the coating layer under long-term UV irradiation. As a desirable progress, luminescent glasses and glass ceramics were reported as good alternatives for the phosphor

---

Z. Shan · D. Chen · Y. Yu · P. Huang · H. Lin · Y. Wang (✉)
State Key Laboratory of Structural Chemistry, Fujian Institute of Research on the Structure of Matter, Chinese Academy of Sciences, Graduate University of Chinese Academy of Sciences, Fuzhou, Fujian 350002, China
e-mail: yswang@fjirsm.ac.cn

powders since they can be formed in plate-like shape to ensure a direct encasement of the UV chip [18–20].

In this article, the $Tb^{3+}$- or $Dy^{3+}$-doped glass ceramics containing $GdF_3$ nanocrystals, which have not yet been reported before, were fabricated. The efficient energy transfers from $Gd^{3+}$ to $Tb^{3+}$ and $Dy^{3+}$ was demonstrated. More significantly, an intense white light emission was observed in the $Dy^{3+}$-doped sample under ultraviolet excitation.

## Experimental

The precursor glasses were prepared with the following composition (in mol%): $44SiO_2–28Al_2O_3–17NaF–11GdF_3$. The $Dy^{3+}$ or $Tb^{3+}$ doping was introduced by the addition of $DyF_3$ or $TbF_3$, respectively, with RE content set from 0.1 to 2.5 mol%. For each batch, about 10 g of raw materials were fully mixed and melted in a covered platinum crucible in air atmosphere at 1400 °C for 30 min, then cast into a brass mold followed by annealing to relinquish the inner stress. The obtained precursor glasses were then heated at 670 °C for 2 h to form glass ceramics through crystallization.

To identify the crystallization phase and determine the mean size of the crystallites, X-ray diffraction (XRD) analysis was carried out with a powder diffractometer (DMAX2500 RIGAKU) using Cu K$\alpha$ radiation ($\lambda = 0.154$ nm). The microstructures of the samples were studied using a transmission electron microscope (TEM, JEM-2010) equipped with an energy dispersive X-ray spectroscope (EDS). The emission and excitation spectra and the decay curves of the samples were recorded on an Edinburgh Instruments FLS920 spectrofluoremeter equipped with both continuous and pulse xenon lamps. All the measurements were carried out at room temperature.

## Results and discussion

XRD patterns of the 0.1 mol% $Dy^{3+}$-doped precursor glass and glass ceramic are shown in Fig. 1. There are only two diffuse humps in the precursor glass, indicative of its amorphous nature. After heat-treated at 670 °C, several intense diffraction peaks ascribed to the hexagonal $GdF_3$ nanocrystals appear [21]. Based on the diffraction peak widths, the mean size ($D$) of the $GdF_3$ crystallites were evaluated to be 16 nm by Scherrer equation:

$$D = \frac{0.9\lambda}{\beta \cos\theta} \tag{1}$$

where $\lambda$ is the X-ray wavelength, $\beta$ the full width at half maximum of the peak, and $\theta$ the diffraction angle. As an example, Fig. 2 presents the typical TEM micrograph of the $GdF_3$-based glass ceramic, which exhibits the homogeneous distribution of the spherical $GdF_3$ nanocrystals with sizes of 13–18 nm in the glass matrix, in consistent with the XRD results. The corresponding selected area electron diffraction (SAED) pattern, shown in the inset of Fig. 2, exhibits the polycrystalline diffraction feature of $GdF_3$.

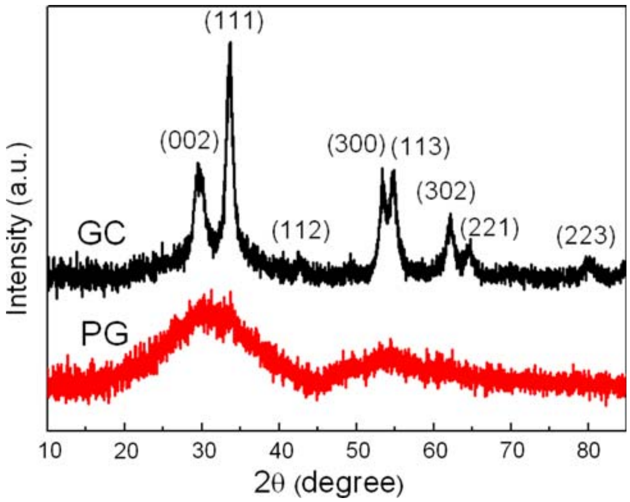

**Fig. 1** XRD patterns of 0.1 mol% $Dy^{3+}$-doped precursor glass (PG) and glass ceramic (GC), respectively

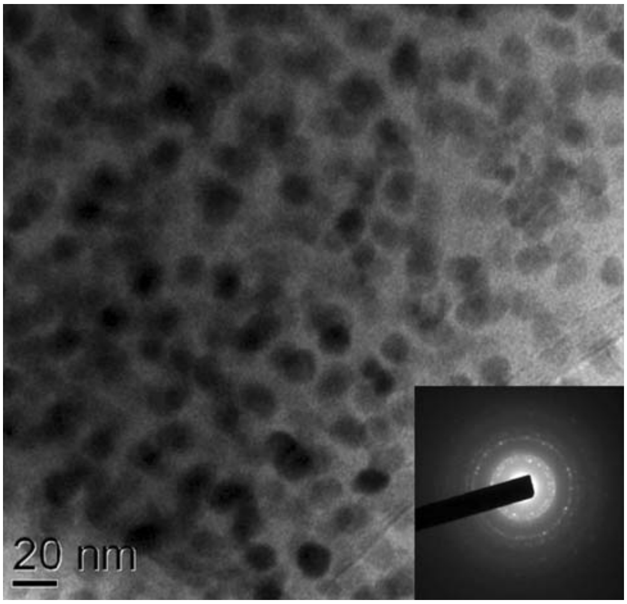

**Fig. 2** TEM micrograph and SAED pattern of 0.1 mol% $Dy^{3+}$-doped glass ceramic

To explore the distribution of RE ions in the glass ceramics, the EDS spectra with a nanosized probe taken from an individual $GdF_3$ nanocrystal and from the glass matrix were measured, respectively, for the glass ceramics doped with $Dy^{3+}$. The spectrum from the nanocrystal,

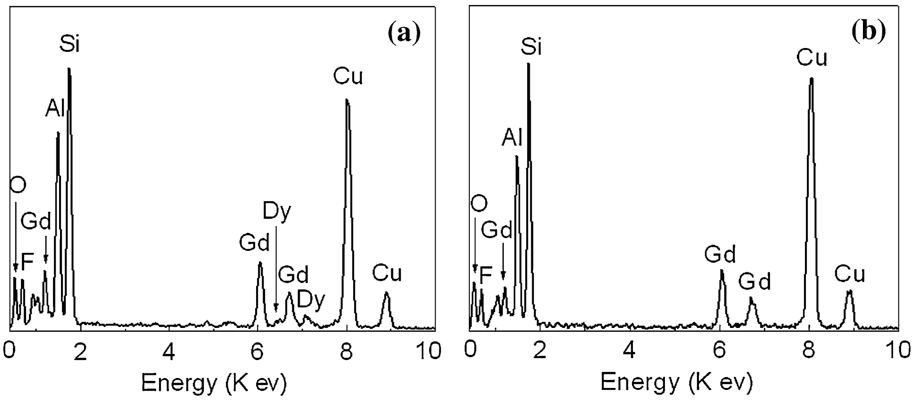

**Fig. 3** EDS spectra taken from **a** an individual $GdF_3$ nanocrystal, and **b** the glass matrix in the 0.1 mol% $Dy^{3+}$-doped glass ceramic

shown in Fig. 3a, exhibits Gd, F, and Dy signals (the Al, Si, and O peaks are attributed to the glass matrix surrounding the nanocrystal, and the Cu ones are originated from the copper grid supporting the TEM specimen), while in the spectrum of the glass matrix presented in Fig. 3b, no Dy signals are detected, indicating that RE ions are mainly concentrated in the $GdF_3$ nanocrystals.

The excitation and emission spectra of the $Tb^{3+}$-doped glass ceramics are presented in Fig. 4. There are two sets of excitation signals appearing in the excitation spectrum shown in Fig. 4a for the 542 nm ($Tb^{3+}$: ${}^5D_4 \rightarrow {}^7F_6$) emission: one consists of several characteristic $Tb^{3+}$ excitation peaks from the ${}^7F_6$ ground state to the indexed excited states, and the other consists of two excitation bands at 273 nm and 311 nm originated from the $Gd^{3+}$: ${}^8S_{7/2} \rightarrow {}^6I_J$ and ${}^8S_{7/2} \rightarrow {}^6P_J$ transitions, respectively. Figure 4b exhibits the emission spectra of the glass ceramics doped with various contents of $Tb^{3+}$ under the excitation of 273 nm ($Gd^{3+}$: ${}^8S_{7/2} \rightarrow {}^6I_J$). There are several intense peaks ranging from 480 to 650 nm ascribing to the $Tb^{3+}$ transitions from ${}^5D_4$ to ${}^7F_J$ ($J = 6, 5, 4, 3$), respectively. These emissions intensify monotonously with increasing of $Tb^{3+}$ content, evidencing an efficient energy transfer from $Gd^{3+}$ to $Tb^{3+}$. The possible energy transfer process is schematically depicted in the RE energy level diagrams shown in Fig. 5. It is worthy to mention that the emissions from the higher excited-state transitions, i.e., ${}^5D_3 \rightarrow {}^7F_J$ ($J = 6, 5, 4, 3, 2$), are also detected. Remarkably, the intensities of these emissions exhibit a converse trend with $Tb^{3+}$ content, i.e.,

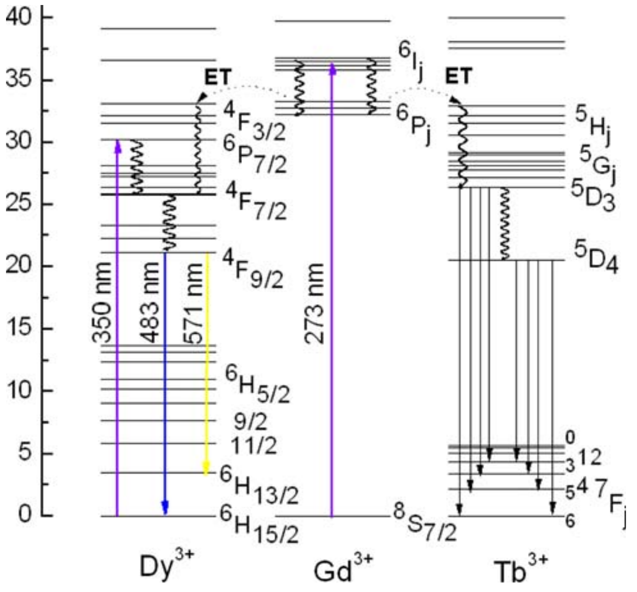

**Fig. 5** Energy-level diagrams of $Gd^{3+}$, $Dy^{3+}$, and $Tb^{3+}$, showing possible processes of energy transfers from $Gd^{3+}$ to $Tb^{3+}$ or $Dy^{3+}$. Solid, dotted, and curved arrows denote optical transitions, energy transfers (ET), and non-radiative transitions, respectively

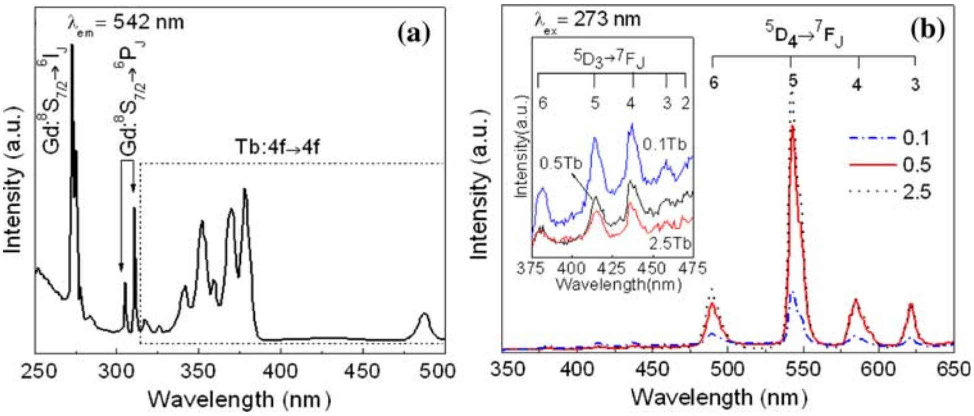

**Fig. 4** Excitation ($\lambda_{em} = 542$ nm) (**a**), and emission ($\lambda_{ex} = 273$ nm) (**b**) spectra of $Tb^{3+}$-doped glass ceramic; inset of (**b**) shows enlarged emission spectra in 375–475 nm region

they decrease with increasing of $Tb^{3+}$ content from 0.1 to 2.5 mol%, as shown in the inset of Fig. 4b, which might be ascribed to the cross-relaxation between $Tb^{3+}$ ions, i.e., $^5D_3 + {}^7F_6 \rightarrow {}^5D_4 + {}^7F_0$ [22]. Since the emission at 542 nm is the strongest one, all the samples display green luminescence visible by the naked eyes.

To demonstrate the potential application of the glass ceramics as the luminescent hosts for W-LEDs, the luminescent performances of the $Dy^{3+}$-doped samples were investigated. Figure 6 depicts the excitation spectrum of the 0.1 mol% $Dy^{3+}$-doped glass ceramic, monitored at 571 nm ($Dy^{3+}$: $^4F_{9/2} \rightarrow {}^6H_{13/2}$). Similar to the case of the $Tb^{3+}$-doped sample, the $Gd^{3+}$ excitation transitions are also detected, demonstrating the occurrence of energy transfer from $Gd^{3+}$ to $Dy^{3+}$ which is described in Fig. 5. However, the excitation peak of $Gd^{3+}$ at 273 nm is much weaker than that of the intrinsic $Dy^{3+}$ at 350 nm. The emission spectra of the 0.1 mol% $Dy^{3+}$-doped precursor glass and glass ceramic under excitation of 350 nm is presented in Fig. 7a. Two intense emission bands centered at 480 nm (blue) and 571 nm (yellow), ascribed to the $^4F_{9/2} \rightarrow {}^6H_{15/2}$ and the $^4F_{9/2} \rightarrow {}^6H_{13/2}$ transitions of $Dy^{3+}$, respectively, are observed. There is a significant change in the intensity ratio of the yellow-to-blue emissions for the glass and glass ceramic. The decreased yellow-to-blue ratio in the glass ceramic is attributed to the $GdF_3$ crystalline environment of $Dy^{3+}$ ions, since the yellow emission originated from the hypersensitive transition of $Dy^{3+}$: $^4F_{9/2} \rightarrow {}^6H_{13/2}$ is strongly influenced by the ligand field of $Dy^{3+}$ [23]. In addition, based on the $Dy^{3+}$ $^4F_{9/2}$ decay curves shown in Fig. 7b, the evaluated $Dy^{3+}$ $^4F_{9/2}$ lifetime for the precursor glass (1.06 ms) is longer than that for the glass ceramic (0.75 ms). Figure 7c presents the Commission International de I'Eclairage (CIE) 1931 chromaticity diagram converted from the emission spectra of the 0.1 mol% $Dy^{3+}$-doped samples. The calculated color coordinate is (0.355, 0.403) for the precursor glass, while it is (0.334, 0.391), much closer to (0.333, 0.333) of the standard equal energy white light illuminate, for the glass ceramic. Significantly, the glass ceramic generates intense

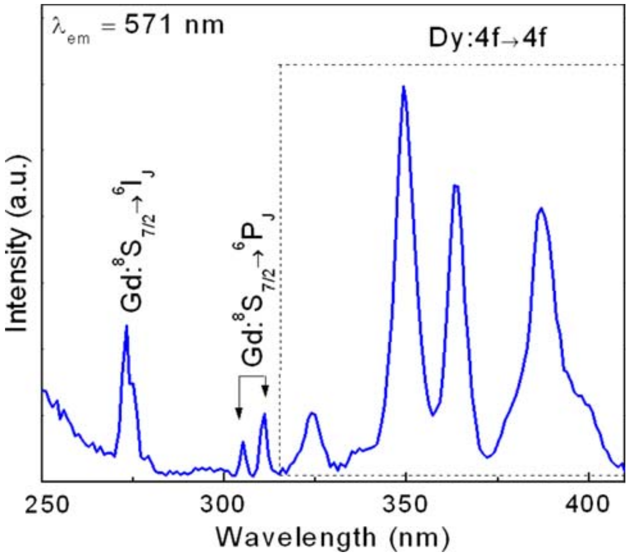

**Fig. 6** Excitation ($\lambda_{em}$ = 571 nm) spectrum of 0.1 mol% $Dy^{3+}$-doped glass ceramic

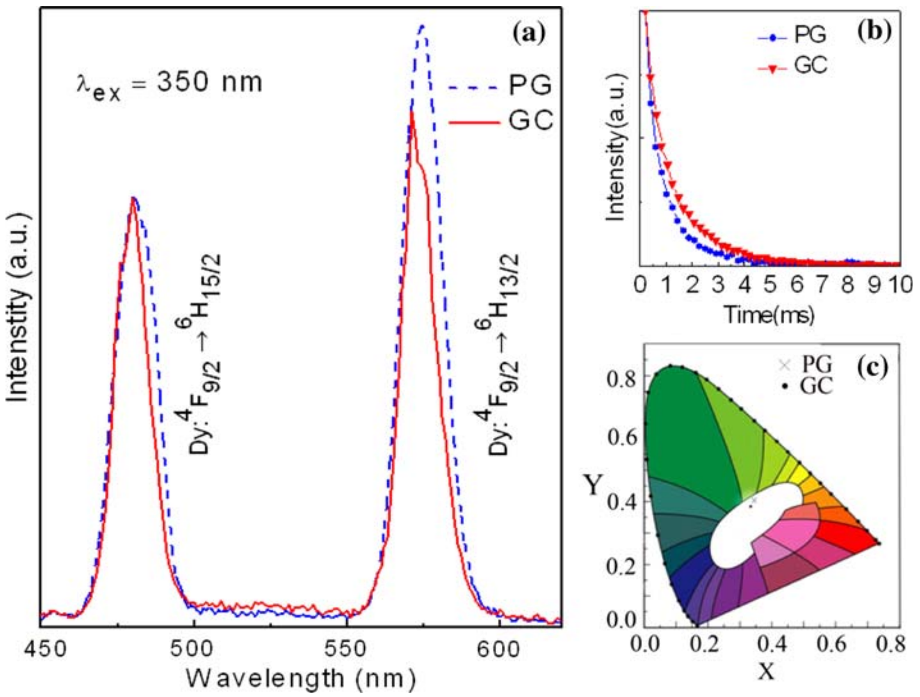

**Fig. 7** Emission ($\lambda_{ex}$ = 350 nm) spectrum (**a**), decay curves (**b**), and CIE 1931 chromaticity diagram (**c**) of 0.1 mol% $Dy^{3+}$-doped precursor glass (PG) and glass ceramic (GC)

white light visible by the naked eyes, indicative of their potential applicability as the luminescent host for W-LEDs.

## Conclusions

The RE-doped transparent oxyfluoride glass ceramics containing hexagonal $GdF_3$ nanocrystals were prepared by melt-quenching and subsequent heating. The efficient energy transfer from $Gd^{3+}$ to $Tb^{3+}$ is evidenced, which resulted in the intense green light emission in the $Tb^{3+}$-doped glass ceramic. The $Dy^{3+}$-doped glass ceramic emits intense white light under UV excitation, demonstrating its potential applicability in the field of W-LEDs.

**Acknowledgements** This study was supported by the National Natural Science Foundation of China (10974201, 50902130), the Natural Science Foundation of Fujian Province (2009J05139), the Knowledge Innovation Program of CAS, and the National Engineering Research Center for Optoelectronic Crystalline Materials (2006K02, 2009KL002).

## References

1. Lahoz F (2008) Opt Lett 33:2982
2. Babu P, Jang K, Kim E, Shi L, Seo H, Rivera-López F, Rodríguez-Mendoza U, Lavín V, Vijaya R, Jayasankar C (2009) J Appl Phys 105:013516
3. Chen D, Yu Y, Huang P, Weng F, Lin H, Wang Y (2009) Appl Phys Lett 94:041909
4. Clara GM, Santos LF, Almeida RM (2002) C R Chim 5:845
5. Wang Y, Ohwaki J (1993) Appl Phys Lett 63:3268
6. Driesen K, Tikhomirov V, G rller-Walrand C, Rodríguez V, Seddon A (2006) Appl Phys Lett 88:073111
7. Dantelle G, Mortier M, Vivien D, Patriarche G (2005) Chem Mater 17:2216
8. Fan X, Wang J, Qiao X, Wang M, Adam J, Zhang X (2006) J Phys Chem B 110:5950
9. Lahoz F, Hernández S, Capuj N, Navarro-Urrios D (2007) Appl Phys Lett 90:201117
10. Pisarski W, Goryczka T, Pisarska J, Ryba-Romanowskis W (2007) J Phys Chem B 111:2427
11. Chen D, Wang Y, Yu Y, Huang P (2007) Appl Phys Lett 91:051920
12. Ye S, Zhu B, Luo J, Chen J, Lakshminarayana G, Qiu J (2008) Opt Express 16:8989
13. Ribeiro S, Diniz R, Messaddeq Y, Nunes L, Aegerter M (1994) Chem Phys Lett 220:214
14. Armaroli N, Balzani V, Barigelletti F, Ward M, McCleverty J (1997) Chem Phys Lett 276:435
15. Park J, Lim M, Kim C, Park H, Park J, Choi S (2003) Appl Phys Lett 82:683
16. Chang C, Chen T (2007) Appl Phys Lett 91:081902
17. Liu X, Lin C, Lin J (2007) Appl Phys Lett 90:81904
18. Zheng Y, Clare A (2005) Phys Chem Glasses 46:467
19. Tanabe S, Fujita S, Yoshihara S, Sakamoto A, Yamamoto S (2005) Proc SPIE 5491:594112
20. Fujita S, Yoshihara S, Sakamoto A, Yamamoto S, Tanabe S (2005) Proc SPIE 5491:594111
21. Chen D, Wang Y, Yu Y, Huang P (2008) J Phys Chem C 112:18943
22. Li Y, Chang Y, Chang Y, Lin Y, Laing C (2007) J Phys Chem C 100:10682
23. Han B, Liang H, Lin H, Chen W, Su Q, Yang G, Zhang G (2008) J Opt Soc Am B 25:2057